Catalysis Today 143 (2009) 86–93

Contents lists available at ScienceDirect

Catalysis Today

journal homepage: www.elsevier.com/locate/cattod

Effect of S-compounds on Pd over $LaMnO_3{\cdot}2ZrO_2$ and $CeO_2{\cdot}2ZrO_2$ catalysts for CH_4 combustion

S. Specchia [a,*], E. Finocchio [b], G. Busca [b], G. Saracco [a], V. Specchia [a]

[a] Dipartimento di Scienza dei Materiali ed Ingegneria Chimica, Politecnico di Torino – Corso Duca degli Abruzzi 24, 10129 Torino, Italy
[b] Dipartimento di Ingegneria Chimica e di Processo "G. Bonino", Università di Genova – Piazzale Kennedy 1, 16129 Genova, Italy

ARTICLE INFO

Article history:
Available online 11 December 2008

Keywords:
Catalytic combustion
Methane
Pd-based catalysts
Accelerated ageing
SO_2 poisoning
FT-IR spectroscopy

ABSTRACT

The ageing effect induced by S-compounds (added as odorants in the natural gas network for safety purposes) over 2% $Pd/LaMnO_3{\cdot}2ZrO_2$ and 2% $Pd/CeO_2{\cdot}2ZrO_2$ catalysts for CH_4 combustion is studied. The catalysts were prepared by solution combustion synthesis (SCS), starting from metal nitrates/glycine mixtures. Basic characterization (XRD, BET, FESEM/EDS, TPD/TPR analysis), FT-IR studies and catalytic activity tests were performed on powder catalysts in fresh status and after accelerated ageing carried out up to 3 weeks (hydro-thermal treatment at 800 °C under a flow of domestic boiler exhaust gases typical composition (9% CO_2, 18% H_2O, 2% O_2 in N_2), also including 200 ppmv of SO_2 to emphasize any poisoning effect). After ageing, 2% $Pd/CeO_2{\cdot}2ZrO_2$ increased its CH_4 combustion half-conversion temperature (T_{50}), regarded as an index of catalytic activity, from 382 °C – recorded for fresh sample – to 490 °C. An unexpected improvement in the overall performance was found instead for 2% $Pd/LaMnO_3{\cdot}2ZrO_2$: T_{50}, in fact, got lowered from 570 °C (fresh sample) to 465 °C (after 3 weeks ageing). S-hydro-thermal treatment induced bulk and surface sulphates formation on all aged samples, with a concentration increasing with the exposure time. The prevailing ageing mechanisms seemed to be the oxidation of Pd metallic clusters, detected over the Ce–Zr system, and the formation of surface-bulk sulphates, the latter destroying the initial crystallographic structure, particularly evident for the La–Mn system. The increased activity of the 2% $Pd/LaMnO_3{\cdot}2ZrO_2$ sample could be explained with the formation of MnO_x, detected via XRD and IR, which is active towards CH_4 combustion.

1. Introduction

In the last decades, the growing importance of natural gas (NG) as a power source increased the efforts to develop efficient and safe combustion systems to respect the ultimate modern climate policy requirements. NG combustion has been widely studied and analyzed in relation to the concentration of pollutants like NO_x and CO, and several solutions have been evaluated to reach new highly efficient and clean combustion appliances [1]. Promising results were obtained with low-environmental-impact premixed metal fibre burners, due to their thermal efficiency and environmental impact superior performance (remarkable NO_x reduction [2]). Coupling radiant-premixed burners with PdO_x/perovskite-based catalysts proved to further improve burners' performance [3]. With such catalysts (attractive for their low cost, thermo-chemical stability at high temperature (900–1100 °C) and catalytic activity [1]) the fuel fraction burnt within or just downstream the burner outlet surface is increased, thus maximizing the radiant heat fraction, cooling the flame temperature and improving the combustion completeness (lower concentration of CO and unburnt HC). Since PdO_x/perovskite-based catalysts are prone to be poisoned by S-compounds [4–6], used as odorants in NG networks, the present work deals with a deep analysis on poisoning mechanisms induced by S-compounds on 2% $Pd/LaMnO_3{\cdot}2ZrO_2$ and 2% $Pd/CeO_2{\cdot}2ZrO_2$ in order to assess and develop catalysts with longer lifetime.

Pd-based ZrO_2-stabilized catalysts were chosen, in line with earlier investigations [7–11], thanks to their very good performance as structured catalysts on pre-mixed metal fibre burners; an attempt was made to exploit ageing/poisoning mechanism on catalyst powders. Pd-based catalysts are well known as excellent catalysts towards NG oxidation [1]. ZrO_2 acts as a structural promoter, in that its presence limits the specific surface area loss caused by prolonged exposure to high temperatures [12]. The simultaneous synthesis of a perovskite phase such as $LaMnO_3$, which was found to be remarkably active towards NG oxidation [13], and of a suitable second oxide with good thermal resistance (e.g. ZrO_2) that can act as

* Corresponding author. Tel.: +39 011 0904608; fax: +39 011 0904699.
E-mail address: stefania.specchia@polito.it (S. Specchia).

0920-5861/$ – see front matter © 2008 Elsevier B.V. All rights reserved.
doi:10.1016/j.cattod.2008.10.035

a structural promoter, was investigated and found beneficial in terms of both higher specific surface area and better resistance to high temperatures [14]. Perovskites are attractive with respect to noble metals, traditionally employed for this kind of application, thanks to their lower cost and the absence of problems such as sublimation and volatilization [15]. The perovskite structure allows for a number of substitutions and compositional modifications, so that different oxidation states for the transition metal are possible, as well as anionic or cationic defectivity [16,17]. However, one of the main drawbacks of perovskites is their limited specific surface area, especially when they are prepared with solid-state reactions between the oxide precursors at high temperatures [17]. The mixed oxide system of $CeO_2{\cdot}ZrO_2$ is also a very promising catalyst: CeO_2 is particularly appreciated as promoter for many employments in the catalytic combustion with noticeable application as automotive exhausts oxidation catalyst [18]. CeO_2 in fact, shows a good capability of changing rapidly its oxidation number from Ce^{3+} to Ce^{4+} state, with a consequent O_2 fast release from its lattice to the nearby species [19,20].

In this work, the solution combustion synthesis (SCS) technique was chosen for the development of the selected catalysts. Powders prepared via SCS generally have higher specific surface areas, as well as pure phases with the desired chemical compositions [21]. The wider the specific surface area, the more effective the Pd dispersion over the carrier and the easier the detection of Pd-carrier synergetic effects. A higher specific surface area would also favour the formation of small-size Pd particles, a key factor for catalytic activity enhancement, as demonstrated recently for the reference Pd/ZrO_2-based catalytic system [12]. Besides, SCS represents an interesting preparation route for other potential advantages: relatively cheap starting reactants (metals nitrates); simple and easily available organic molecules as internal fuel; highly exothermic and self-sustaining reactions. Furthermore, a SCS-based technique for the deposition of perovskite catalysts on the metallic fibre mats of premixed burners was successfully developed recently [8] to prepare structured catalysts.

2. Experimental

2% $Pd/LaMnO_3{\cdot}2ZrO_2$ and 2% $Pd/CeO_2{\cdot}2ZrO_2$ powdered catalysts were prepared via SCS, a process based on the oxidation of an organic fuel, like glycine, which provides the necessary synthesis heat [2,22]. Metal nitrates of La, Mn, zyrconyl and Pd in one case, of Ce, zyrconyl and Pd in the other one (Aldrich, 99% purity), were used as precursors, acting as oxidizers of glycine in solution. The organic molecule plays a double role: (i) by forming complexes with metal cations in aqueous solution, it guarantees good solution homogeneity, preventing the preferential precipitation of ionic species; (ii) it reacts with the precursors (metal nitrates). The overall combustion reactions can be written as

$$La(NO_3)_3 + Mn(NO_3)_2 + 2ZrO(NO_3)_2 + Pd(NO_3)_2 + \tfrac{56}{9}COOH{-}CH_2{-}NH_2 \rightarrow Pd(LaMnO_3 \cdot 2ZrO_2) + \tfrac{112}{9}CO_2 + \tfrac{140}{9}H_2O + \tfrac{155}{18}N_2 \quad (1)$$

$$Ce(NO_3)_3 + 2ZrO(NO_3)_2 + Pd(NO_3)_2 + \tfrac{46}{9}COOH{-}CH_2{-}NH_2 \rightarrow Pd(CeO_2 \cdot 2ZrO_2) + \tfrac{92}{9}CO_2 + \tfrac{115}{9}H_2O + \tfrac{127}{18}N_2 \quad (2)$$

The precursors and the fuel, dosed in the stoichiometric amount, were dissolved in distilled water and the resulting solution, thoroughly stirred to ensure complete dissolution of all reagents, was then transferred in a ceramic dish and placed into an electric oven set at 450 °C. After water evaporation and a significant increase in the system viscosity, the heat released in the fast reaction allowed the formation of the catalytic powders. Subsequently, the as-prepared powders were calcined in oven at 800 °C for 2 h in still air [11], so as to favour decomposition of the eventually unreacted nitrate precursor. The obtained oxidized Palladium form (PdO), which is stable at the lower temperatures and thermally decomposes into metallic Pd when temperature is raised above 800 °C, is generally regarded as the more active phase [23].

Since Pd/oxide-based catalysts are prone to be poisoned by Sulphur compounds (normally used as odorants in natural gas networks), the catalytic powders were kept in an electric tubular oven at 800 °C (a thermocouple was used to monitor the furnace temperature) under a flow rate with typical domestic boiler exhaust composition (9% CO_2, 18% H_2O, 2% O_2 in N_2); 200 ppmv of SO_2 were added on purpose. The latter value was chosen several times higher than the odorant supplementary concentration in commercial natural gas (about 8 ppmv, in Italy, as THT) so as to accelerate any possible poisoning effect [5,10,24]. Earlier Sulphur poisoning studies on perovskite catalysts showed that the basic poisoning mechanism under catalytic combustion conditions was chemisorption of SO_2/SO_3 species generated by combustion of whatever Sulphur-organic compound present in the feed (e.g. odorants) [5]. Particularly, it was demonstrated that the direct presence of SO_2 or of the THT odorant in the feed did not lead to a significantly different ageing effect, provided the overall Sulphur content remaining the same. SO_2/SO_3 species, in fact, resulted from the total oxidation of S-containing organics during the combustion process [4]. For this reason only ageing runs with a SO_2-laden flow were accomplished. The catalyzed burners were continuously aged up to 3 weeks: for a domestic boiler, such operating time in 200 ppmv SO_2 atmosphere may be considered equivalent to a utilization life time of approximately 3 years under real operation [11]. The as-prepared catalysts were completely characterized at fresh status and after each week of ageing (F/1W/2W/3W samples).

The catalytic activity towards NG oxidation of the fresh and aged catalytic powders was tested in a lab-scale fixed-bed micro-reactor (temperature programmed combustion, TPC): 0.1 g of catalyst mixed with 0.9 g of SiO_2, sandwiched between two quartz wool layers, were inserted in a quartz tube (4 mm ID). The obtained micro-reactor was placed into a PID regulated electrical oven [9] and fed with 50 N cm^3 min^{-1} of a gaseous mixture containing 2% CH_4 and 16% O_2 in He. The micro-reactor temperature was measured by a K-thermocouple placed inside the catalytic bed. Starting from 800 °C, the oven temperature was decreased at 2 °C min^{-1} rate and the outlet CO_2, CO, CH_4 and O_2 concentrations were determined by a continuous analyzer (NDIR and paramagnetic Uras 14, ABB) to evaluate CH_4 conversion. The half-conversion temperature (T_{50}) was considered as an index of the powders catalytic activity.

The crystal phases and grain size of the various catalysts were detected by X-ray diffraction (Philips PW1710 apparatus equipped with a monochromator for the Cu Kα radiation; markers located according the PcpdfWin database).

The morphology of the powders in the fresh and aged status was studied using a Scanning Electron Microscope (FESEM Leo 50/50 VP with Gemini column).

The surface area and the pore size distribution of all samples were determined by Nitrogen adsorption at the liquid N_2 temperature in a Micrometrics ASAP 2010 M instrument. The surface area was determined according to the Brunauer–Emmett–Teller theory; the samples were degassed in vacuum for at least 4 h at 250 °C before analysis.

Temperature programmed desorption (TPD) and temperature programmed reduction (TPR) tests (Thermoquest TPD/R/O 1100

Series, Thermo Finningan analyzer, equipped with a thermal conductivity detector TCD) were employed to investigate the O_2 desorption with temperature and to quantify the presence of PdO on the catalysts' surface on fresh and aged samples. To perform calculations on PdO amount, reference supports of $LaMnO_3{\cdot}2ZrO_2$ and $CeO_2{\cdot}2ZrO_2$ without noble metal were also employed. TPR tests were performed by firstly flowing 10 N cm^3 min^{-1} of 5% H_2 in Ar, increasing the temperature from 50 to 900 °C at 10 °C min^{-1} to evaluate the H_2 consumption. Then an oxidation treatment was performed by flowing 40 N cm^3 min^{-1} of pure O_2 increasing the temperature from 25 to 750 °C at 40 °C min^{-1} followed by cooling to room temperature in the same oxidizing atmosphere. With the catalysts completed oxidized, TPR tests were performed again by flowing once more 10 N cm^3 min^{-1} of 5% H_2 in Ar, increasing the temperature from 50 to 900 °C at 10 °C min^{-1} to evaluate the new H_2 consumption. Mathematical calculations on the PdO oxide percentage were accomplished by considering the initial and adsorbed volumes of gas, the catalyst amount and the noble metal percentage.

Infrared spectroscopy (Nicolet Nexus FT instrument) was also assessed on all fresh/aged samples: pure catalyst powders were pressed in self-supporting tablets (20 mg average weight) and treated in vacuum at several temperatures in IR cell connected to a gas management apparatus. Fresh and aged catalysts were outgassed at 500 °C and cooled at liquid N_2 temperature before CO adsorption. 10 torr of CO were introduced in the IR cell to saturate catalysts surface sites. IR spectra were recorded from −130 °C to room temperature. In the spectra of adsorbed CO, the activated surface was subtracted.

3. Results and discussion

Fig. 1 shows all the TPC results of fresh and poisoned 2% Pd/$LaMnO_3{\cdot}2ZrO_2$ and 2% Pd/$CeO_2{\cdot}2ZrO_2$ catalysts. A synopsis of the typical $T_{10}/T_{50}/T_{90}$ is presented in Table 1. The performance of 2% Pd/$LaMnO_3{\cdot}2ZrO_2$ improved with ageing showing the best results in the 2W sample, after a first slight decay in 1W sample. On the contrary, the performance of 2% Pd/$CeO_2{\cdot}2ZrO_2$ remained stable till 1 week, with a decline increasing with time on 2W and 3W samples. 2W and 3W samples of both catalysts presented in a slight form the typical Pd/PdO hysteresis phenomenon close to 600 °C.

The XRD spectra for as-synthesized fresh and aged 2% Pd/$LaMnO_3{\cdot}2ZrO_2$ and 2% Pd/$CeO_2{\cdot}2ZrO_2$ powders are presented in Fig. 2. Considering the 2% Pd/$LaMnO_3{\cdot}2ZrO_2$ samples, weak diffraction peaks of tetragonal ZrO_2 and orthorhombic $LaMnO_3$ were detected only in F/1W samples, where it was possible to notice the simultaneous growth of both phases; ZrO_2 phase got segregated with ageing. The presence of $LaO_2{\cdot}SO_4$ with ageing

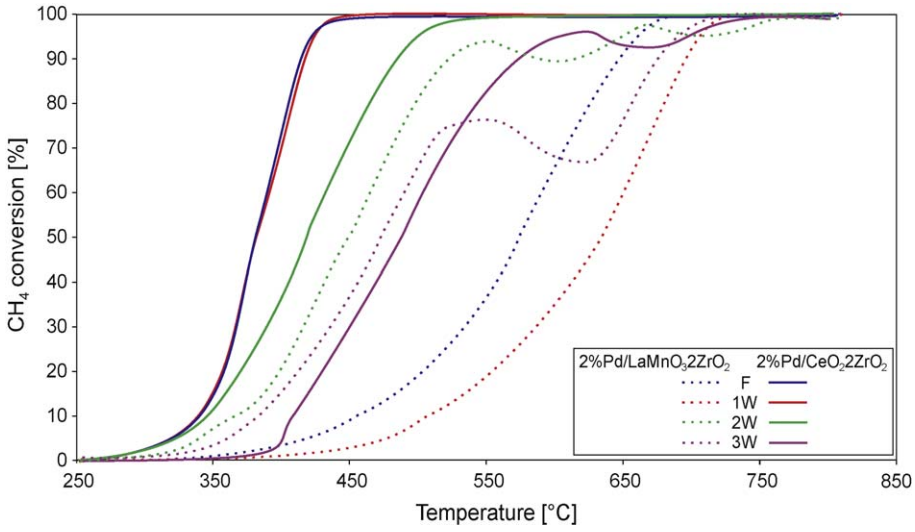

Fig. 1. TPC curves of fresh and aged (1 week: 1W; 2 weeks: 2W; 3 weeks: 3W) 2% Pd/$LaMnO_3{\cdot}2ZrO_2$ and 2% Pd/$CeO_2{\cdot}2ZrO_2$ catalysts.

Table 1
Characterization of the fresh and aged samples (1 week, 2 weeks and 3 weeks) of 2% Pd/$LaMnO_3{\cdot}2ZrO_2$ and 2% Pd/$CeO_2{\cdot}2ZrO_2$ catalysts (n.d.: not determined).

	2% Pd/$LaMnO_3{\cdot}2ZrO_2$				2% Pd/$CeO_2{\cdot}2ZrO_2$			
	F	1W	2W	3W	F	1W	2W	3W
T_{10} (°C)	450	500	360	375	340	336	345	409
T_{50} (°C)	570	625	450	465	382	383	421	490
T_{90} (°C)	645	690	550	550	429	419	498	598
BET (m^2/g)	132.5	69.8	21.6	20.3	74.6	65.8	34.8	21.5
Grain size (nm)	45[a], 10[b]	88[a], 9[b]	–	–	56[c], 11[b]	75[c], 10[b]	85[c], 12[b]	96[c], 11[b]
Desorbed O_2 (μmol/g)	233.3	205.8	186.6	183.2	54.2	49.8	52.7	51.9
α-O_2 (μmol/g)	–	30.1	2.5	2.3	46.1	39.9	10.5	-
β-O_2 (μmol/g)	233.3	175.7	184.1	180.9	8.1	9.9	42.2	51.9
T_p (°C)	960	935[d]	860	860	535	550	650	790
PdO (%)[e]	29.5	41.5	n.d.	78.5	28.6	34.4	n.d.	82.6

[a] Referred to $LaMnO_3$.
[b] Referred to ZrO_2.
[c] Referred to CeO_2.
[d] Average value between peaks @ 840/1030 °C.
[e] From TPR data.

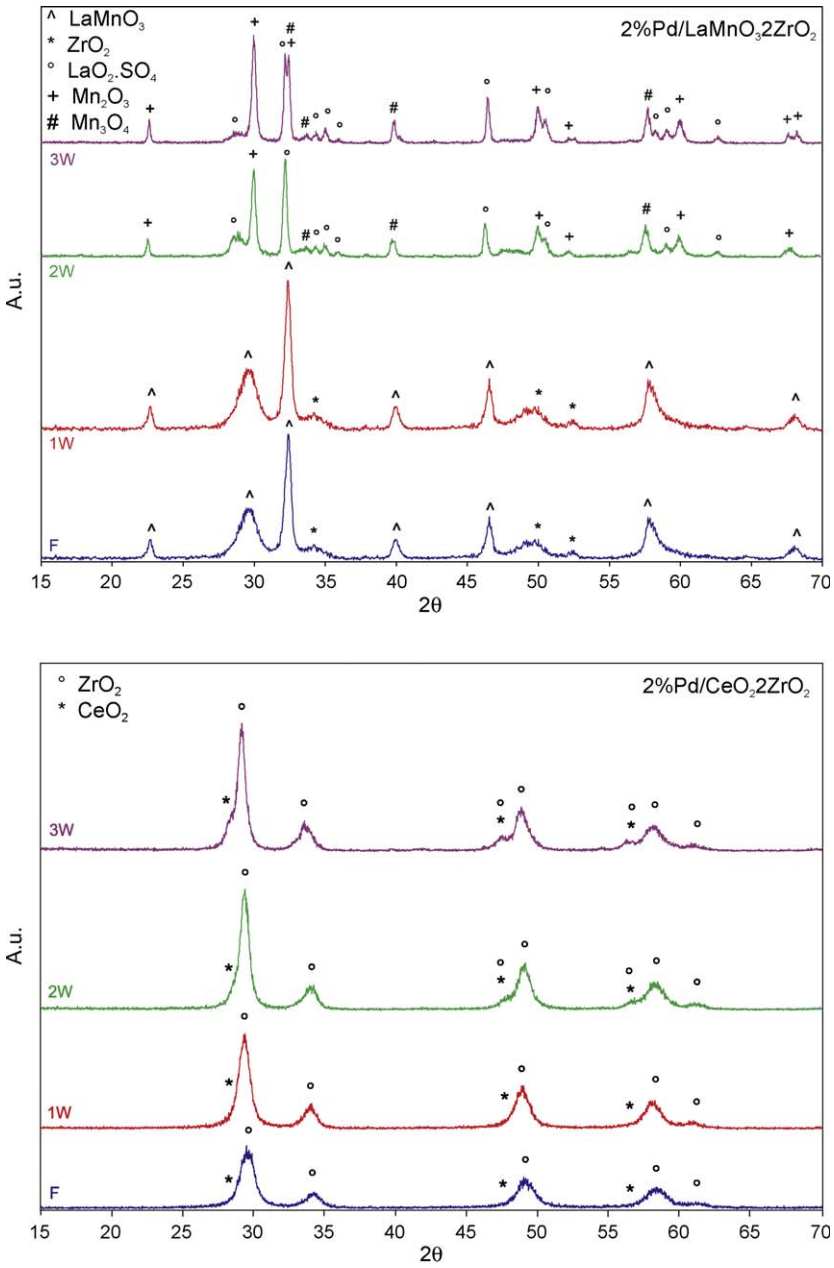

Fig. 2. XRD patterns of fresh and aged (1 week: 1W; 2 weeks: 2W; 3 weeks: 3W) 2% $Pd/LaMnO_3{\cdot}2ZrO_2$ and 2% $Pd/CeO_2{\cdot}2ZrO_2$ catalysts.

(2W/3W) was detected (in literature, sometimes perovskites poisoning by SO_2 is due to the formation of sulphate and their amount accumulated at the surface in form of $La_2(SO_4)_3$ [25]), so as the appearance of Manganese oxides (Mn_2O_3 and Mn_3O_4) with ageing on samples 2W/3W (the sulphates formation is usually accompanied by segregation of simple oxides [25]). The Mn oxides, well known in literature for their good catalytic activity towards CH_4 combustion [26–31], could be probably responsible of the enhanced catalytic activity of 2% $Pd/LaMnO_3{\cdot}2ZrO_2$ with ageing, recorded during the TPC tests. Considering instead the 2% Pd/$CeO_2{\cdot}2ZrO_2$ samples, in agreement with the composition (CeO_2:ZrO_2 = 1:2), the fresh sample crystallized as the tetragonal phase. The aged samples preserved the crystalline structure obtained after SCS synthesis with an increasing presence of a cubic CeO_2-rich phase that segregated from the initial tetragonal crystalline structure. The phenomenon was well distinguishable in the 3W sample, after 3 weeks of ageing treatment. No diffraction peaks of either Pd or PdO were detected in both systems, in agreement with the small loading (2%, w/w) and a sign that Pd dispersion was satisfactory.

The FESEM images reported in Fig. 3 show that for both catalytic systems, the fresh powders exposed a spongy structure, perforated waffles with nanometric pores and complex network configuration. After 1 week of treatment, the morphology changed radically exhibiting a notched surface. Sintering phenomena occurred after 2 weeks of ageing: 2W and 3W samples of both catalysts, in fact, showed a smooth surface with micro porosity in a range of about 1 μm. Moreover, Pd clusters with dimensions less than 100 nm are visible, especially on 2W and 3W samples of 2% $Pd/LaMnO_3{\cdot}2ZrO_2$.

The BET values, reported in Table 1 together with the mean grain size calculated via the Scherrer equation [32], were very high (strongly related to the synthesis method that allows to process powder with high surface area [2]), in particular for the 2% Pd/$LaMnO_3{\cdot}2ZrO_2$ in the fresh status. Both the catalysts showed a BET

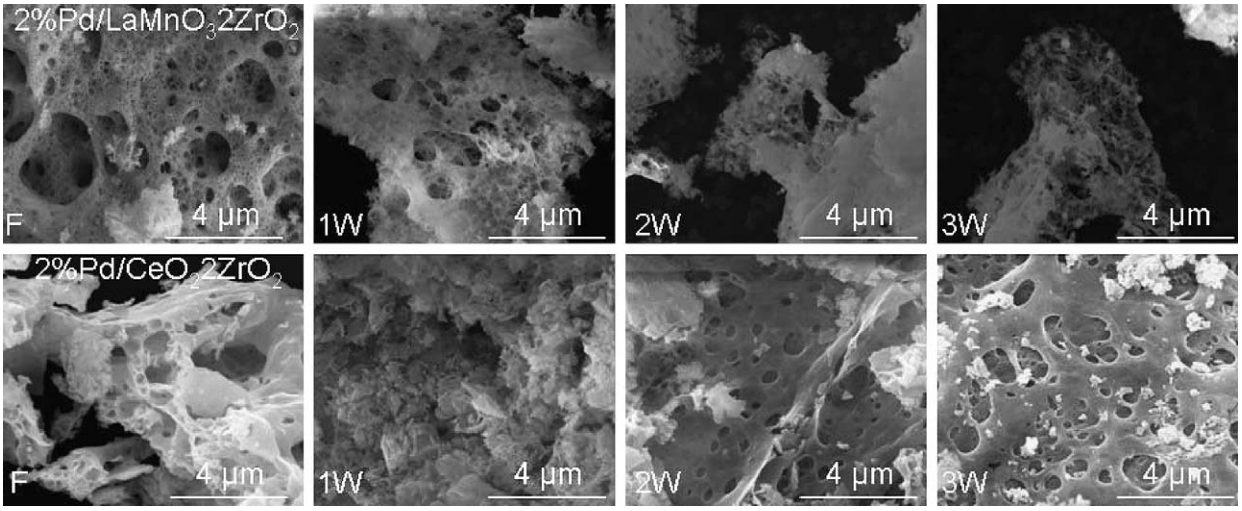

Fig. 3. FESEM micrographs of fresh and aged 1 week: (1W; 2 weeks: 2W; 3 weeks: 3W) 2% $Pd/LaMnO_3{\cdot}2ZrO_2$ and 2% $Pd/CeO_2{\cdot}2ZrO_2$ catalysts.

area worsening with ageing, due to a sintering effect, according also with FESEM analysis, and an increase of the mean grain size. Particularly, the 2% $Pd/LaMnO_3{\cdot}2ZrO_2$ catalyst presented phase segregation: it was indeed not anymore possible to evaluate the mean grain size on 2W and 3W samples. TPR results are reported in Table 1 as percentage of reducible Pd oxides (assuming the PdO stoichiometry) present on each catalytic sample. It is possible to notice how the PdO percentage increased upon ageing: especially for the $LaMnO_3{\cdot}2ZrO_2$ catalysts, this should be explained with the formation of Mn oxides with ageing (enlightened by both XRD analysis and FT-IR studies) which are known to increase the mobility of lattice Oxygen favouring thus the PdO phase stability [26,28]. It is worthy to note that the amount of Oxygen calculated from TPD and TPR data is different but in the same order of magnitude, suggesting that different types of Pd oxides may exist.

The obtained O_2 TPD curves are drawn in Fig. 4. As evident also from Table 1, the 2% $Pd/LaMnO_3{\cdot}2ZrO_2$ catalyst desorbed higher O_2 moles per unit mass, compared to 2% $Pd/CeO_2{\cdot}2ZrO_2$. The total specific moles reduced with ageing and the desorption peak temperature (T_p, assumed as an index of the desorption mean temperature) shifted towards lower values, but always above 600 °C (limit value between α- and β-O_2 species [33]). The 2% $Pd/CeO_2{\cdot}2ZrO_2$ instead, maintained practically the same desorption performance (52.2 μmol g^{-1} ± 4.2%), with a shift of the T_p towards higher values with the ageing. Comparing the TPD and TPC tests

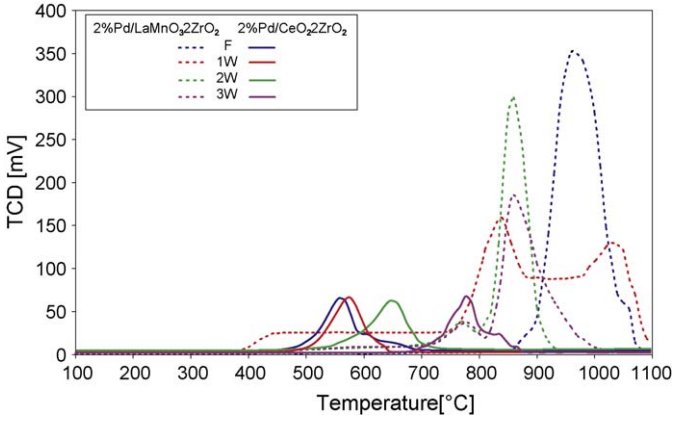

Fig. 4. TPD curves of fresh and aged (1 week: 1W; 2 weeks: 2W; 3 weeks: 3W) 2% $Pd/LaMnO_3{\cdot}2ZrO_2$ and 2% $Pd/CeO_2{\cdot}2ZrO_2$ catalysts.

results, it appears a tight link between the O_2 desorption temperature and the catalytic activity of the two catalysts: the lower the O_2 desorption temperature range (see the T_p values), the higher the catalytic activity toward CH_4 combustion. The trend of T_{90} (combustion TPC) and T_p (O_2 desorption TPD) are indeed in close agreement.

Skeletal IR spectra of the fresh and aged catalysts are reported in Fig. 5. The IR spectra of the fresh 2% $Pd/CeO_2{\cdot}2ZrO_2$ sample were typical of the CeO_2–ZrO_2 system in solid solution. Apparently ageing procedures induced only a small shift of the IR absorption maximum towards higher frequencies [34], in agreement with the CeO_2–ZrO_2 phase segregation observed by XRD. Following ageing for 1 week and 2 weeks another very weak and broad component was growing in the skeletal IR spectra around 1100 cm^{-1}, likely due to bulk sulphate species. The skeletal spectra of fresh and aged 2% $Pd/LaMnO_3{\cdot}2ZrO_2$ catalysts are also reported in Fig. 5. The fresh catalyst spectrum showed a broad absorption growing from 700 to 400 cm^{-1}, with an evident shoulder at 500 cm^{-1}, characterizing the perovskite structure. Ageing entailed the growth of a shoulder at 597 cm^{-1} already evident in the 1W sample spectrum, which became the main band of the spectra recorded following 2 and 3 weeks treatments. In the 2W and 3W sample spectra three main components were finally detected: at 597, 500 and 418 cm^{-1} with a shoulder at 750 cm^{-1}. These features suggested that oxides species were formed, thus confirming results from XRD. In particular, the shoulder at 750 cm^{-1} and the component around 500 cm^{-1} were assigned to Zirconia species (i.e. $mZrO_2$ [35]); whilst the band at 597 cm^{-1}, and another component around 500 cm^{-1} were due to Mn oxides, namely Mn_2O_3 [36], which segregated during ageing. In parallel, in the region 1150–1000 cm^{-1}, weak bands growth in the aged samples spectra, due to sulphate species was observed, as discussed in the section below.

Surface species spectra are reported in Fig. 6, recorded following pure powders outgassing at 500 °C. The fresh 2% $Pd/CeO_2{\cdot}2ZrO_2$ sample spectrum showed two broad and strong bands centred at 1508 and 1406 cm^{-1} due to stretching modes of the CO_3 groups belonging to surface carbonate species. These species were stable at the surface up to 500 °C. A sharp band at 2300 cm^{-1} was due to molecular CO_2 trapped in the catalyst structure. Following ageing, the striking feature of the spectra was the disappearing of the carbonate species, whose IR bands were still detectable, although weaker, in the 1W sample spectrum, but completely disappeared in the 2–3W samples spectra. In 1W sample spectrum, new, sharp components at 1340 and 1280 cm^{-1} appeared, superimposed to

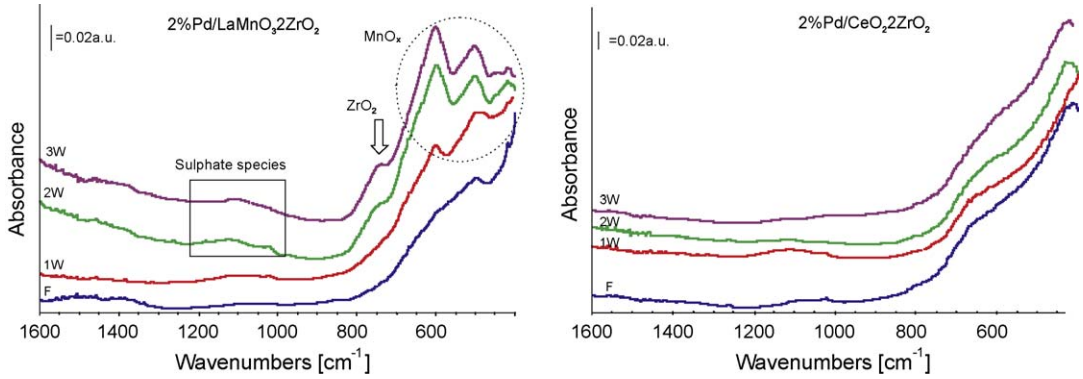

Fig. 5. FT-IR spectra of the skeletal region of fresh and aged 2% $Pd/LaMnO_3{\cdot}2ZrO_2$ and 2% $Pd/CeO_2{\cdot}2ZrO_2$ catalysts.

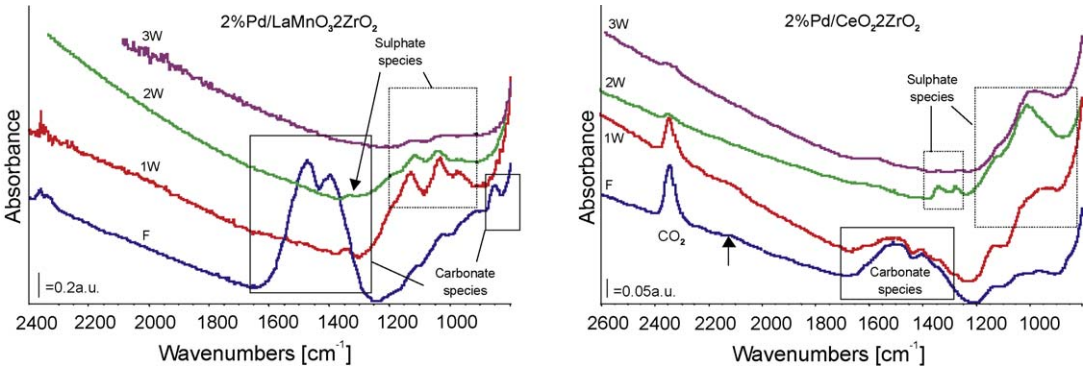

Fig. 6. FT-IR surface species spectra of fresh and aged (1 week: 1W; 2 weeks: 2W; 3 weeks: 3W) 2% $Pd/LaMnO_3{\cdot}2ZrO_2$ and 2% $Pd/CeO_2{\cdot}2ZrO_2$ catalysts outgassed at 500 °C.

the bands due to residual carbonate species, together with a complex and strong absorption centred at 1000 cm^{-1}, with a shoulder around 1100 cm^{-1}. An absorption tailing to lower frequencies could be also detected. In spectra 6.2W and 6.3W these new bands were slightly modified and the maximum shifts below 1000 cm^{-1}. Following literature results [37], these complex bands could be assigned to Sulphur-containing species. The band around 1340 cm^{-1} was due to S=O stretching mode of a surface (mono-oxo) sulphate species, having some covalent character, while it has been suggested that the band at 1260 cm^{-1} can be assigned to a similar sulphate surface species having different coordination (di-oxo species). An evidence in favour of such assignation came from the behaviour of these band which appeared together following 1 week ageing, reached their maximum following 2 weeks ageing then decreased in intensity. This effect could be explained considering surface sulphates formed in a first poisoning step, then diffusing in the bulk. Bands below 1200 cm^{-1} are typically due to S–O stretching modes of ionic sulphates. In particular, bulk sulphates species over 2% $Pd/CeO_2{\cdot}2ZrO_2$ systems should be characterized by a complex massif absorption above 1100 cm^{-1} with pronounced shoulder around 1070 and 990 cm^{-1} [37]. The broad absorption tailing towards 900 cm^{-1}, could be assigned to sulphite species, possibly formed by decomposition of sulphate in our experiment conditions, i.e. heating in vacuum.

Following 3 weeks ageing sulphate species appeared to be mainly bulk-like species. On the other side, it is known that over these Ceria–Zirconia mixed oxides, the high ageing temperature and the presence of Ceria favour bulk sulphate formation, while only surface sulphate species are reported to form over Zirconia [38]. No evidence can be found of $PdSO_4$, whose diagnostic band falls around 1430 cm^{-1} [39]. Also in the spectrum of 2% $Pd/LaMnO_3{\cdot}2ZrO_2$ fresh catalyst broad and strong bands centred at 1505 and 1400 cm^{-1}, and a weaker component at 850 cm^{-1}, were due to stretching and deformation modes of the surface carbonate species CO_3^{2-} group. After 1 week ageing, carbonate species completely disappeared over this surface and sulphate species could be detected, characterized by a weak band at 1340 cm^{-1}, due to S=O stretching mode of a surface sulphate and three strong peaks at 1130, 1031 and 973 cm^{-1} assigned to S–O stretching vibrations of ionic sulphate species, close to the frequencies of "subsurface" sulphates described for MgO-promoted $LaMn_{0.5}Mg_{0.5}O_3$ perovskites [40].

Bulk sulphate species were prevailing after 2 and 3 weeks ageing and were characterized by a complex absorption whose maxima were centred at 1116 (with a shoulder at 1190 cm^{-1}) 1040 and 980 cm^{-1}. Rosso et al. [40] reported bulk sulphate to form in a second stage of the catalyst ageing/poisoning, when diffusion into the bulk of surface and subsurface sulphate is activated. XRD diffraction data revealed that in the 2 weeks sample mostly La sulphate were formed.

In parallel, IR light transmission of the catalyst disks decreased following ageing treatments and increasing grain size, to a point where (following 3 weeks ageing) the transmitted light was around 1%. This is the reason why sulphate species bands were barely visible in the spectrum 6.3W.

Comparing the spectra of the two catalyst series some conclusions on support ageing can be drawn:

(i) First, for both catalysts families, IR surface spectra analysis on fresh and poisoned catalysts evidenced a strong competition between formation of carbonate surface species, prevailing over fresh samples, and surface and bulk sulphate species, widespread over the 2W and 3W poisoned catalysts. Prolonged poisoning seems to favour bulk sulphates formations, due to diffusion mechanisms in the catalyst structure. This behaviour can be ascribed to the stronger acidity of Sulphur oxides much

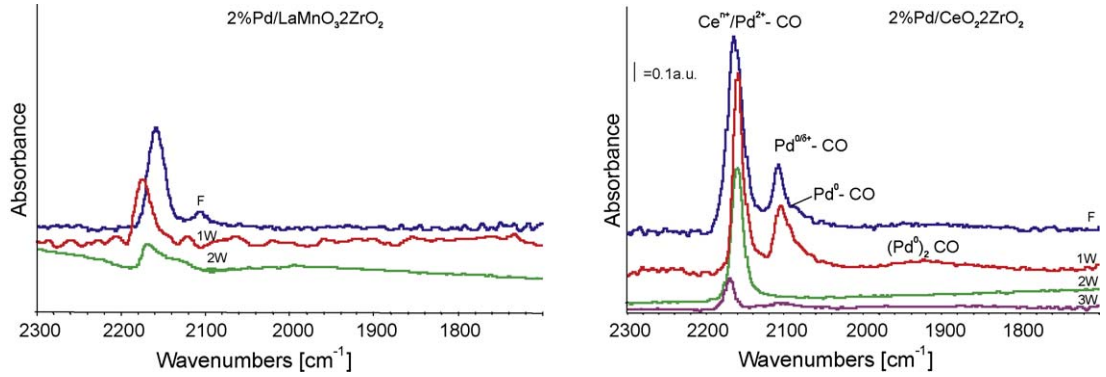

Fig. 7. FT-IR spectra of the surface species arising from low temperature CO adsorption over fresh and aged (1 week: 1W; 2 weeks: 2W; 3 weeks: 3W) 2% $Pd/LaMnO_3{\cdot}2ZrO_2$ and 2% $Pd/CeO_2{\cdot}2ZrO_2$ catalysts outgassed at 500 °C.

more relevant than that of Carbon dioxide and the consequent competition between CO_2 (more abundant) and SO_x (more acidic) adsorption and to competition between CO_2 and SO_2 adsorption on the same basic surface sites followed by ionic sulphate formation with catalysts "basic" components.

(ii) The formed bulk sulphate was stable following outgassing at increasing temperature up to 500 °C. Clearly, the properties of the support were strongly affected by sulphate formations: IR experiments evidenced also the segregation of oxide phases especially in the case of the 2% $Pd/LaMnO_3{\cdot}2ZrO_2$ catalysts. Formation of sulphate was reported to be accompanied by segregation of simple oxides over other perovskite based catalysts, allowing extensive chemical modifications, and this is clearly a phenomenon which makes difficult the evaluation of catalyst deactivation [25].

Another diagnostic parameter is the ratio surface/bulk-like sulphates (i.e. $I_{1350\,cm^{-1}}/I_{\approx1100\,cm^{-1}}$) which is slightly higher in the aged 2% $Pd/CeO_2{\cdot}2ZrO_2$ spectra than aged 2% $Pd/LaMnO_3{\cdot}2ZrO_2$ spectra pointing out an increased surface species sulphate formation over the former catalyst. The metal oxidation state at these surfaces was evaluated through low temperature CO adsorption (Fig. 7).

Over 2% $Pd/CeO_2{\cdot}2ZrO_2$, CO adsorption tests showed Pd highly dispersed on fresh catalyst surfaces. Metal clusters strongly interacting with the support and corresponding to $Pd^{0/\delta+}$ species (carbonyl band at ~2160 cm^{-1}), together with larger Pd^0 particles (carbonyl band at ~2090 cm^{-1}) due to linearly coordinated CO, were detected. Another broad and weak absorption centred at 1930 cm^{-1} is due to CO bridging over Pd^0. Its presence suggests the formation of larger Pd particles following the ageing procedure. At decreasing coverages, the former band intensity decreased (spectra not reported here), confirming the assignment proposed to a species having a partially ionic character, and the wave number did not change, pointing out that no dipole–dipole coupling occurred. This effect is typical of very dispersed metallic systems. CO coordinated over either Pd and support ions was also revealed by the sharp and strong band in 2165–2140 cm^{-1} range [41,42]. In the spectrum recorded after 1 week ageing the main features were the same discussed above: one sharp and strong band at 2159 cm^{-1} due to CO adsorbed over support Cerium ions and, possibly, Pd ions and a sharp band at 2104 cm^{-1}, tailing towards lower wave numbers, due to CO over Pd metallic clusters. After 2 weeks, Pd metal particles were not anymore available to CO coordination and the main band of the IR spectrum was due to CO coordinated over ionic species (either residual Pd or support ions). Following 3 weeks ageing all the carbonyl bands were strongly reduced in intensity.

CO adsorption over the fresh 2% $Pd/LaMnO_3{\cdot}2ZrO_2$ catalyst gave rise to a main strong IR band at 2153 cm^{-1} (Fig. 7). This band is assigned to CO coordinated over exposed ions of the support but can also be partly assigned to CO coordinated over Pd ions. The broad band at 2105 cm^{-1} was due to CO linearly coordinated over $Pd^{0/\delta+}$ clusters, as described above. Following ageing (both 1 week and 2 weeks), just one peak at 2166 cm^{-1} was detectable, or barely detectable in the case of 2-weeks aged catalyst, and was due to CO coordinated over ions of the support. A shoulder at 2136 cm^{-1} could be detected in the subtraction spectrum of 2 weeks aged catalyst, likely assignable to Pd ions. For CO adsorbed over the 3W-aged catalyst, bands in the limit of the noise were detected (the spectrum is not reported here).

Thus, for 2% $Pd/CeO_2{\cdot}2ZrO_2$, the decrease in catalytic activity seems to be mainly due to progressive oxidation of dispersed Pd species, Pd metal particles seeming to be not anymore accessible to CO coordination. The metal particles over the 2% $Pd/LaMnO_3{\cdot}2ZrO_2$ seem to disappear continuously during ageing. This effect was likely due to some sulphate deposits which hindered metal particles access. Pd ions could still coordinate CO, but it was not possible to discriminate the corresponding IR peak from the peak due to CO adsorbed over support ions.

4. Conclusions

SCS was successfully employed for the synthesis of 2% $Pd/LaMnO_3{\cdot}2ZrO_2$ and 2% $Pd/CeO_2{\cdot}2ZrO_2$ catalysts for NG combustion. The powders were characterized after increasing thermal ageing and S-compounds poisoning treatment. On 2% $Pd/LaMnO_3{\cdot}2ZrO_2$, an increased catalytic activity towards NG combustion with ageing was detected, probably supported by Mn oxides formation. Moreover, subsurface and bulk sulphate formation was detected with ageing; phase segregation occurred; Pd metal species were not anymore available for CO coordination. On the contrary, on 2% $Pd/CeO_2{\cdot}2ZrO_2$ a worsening of the catalytic activity was detected with ageing. Prevailing ageing mechanisms seemed to be Pd metallic clusters oxidation detected over the Ce–Zr system, and surface-bulk sulphates formation, the latter destroying the initial crystallographic structure. Prolonged tests with radiant premixed catalytic burners lined with the developed catalyst are under investigation to verify the performance of the developed catalytic material also in the structured form.

References

[1] P. Forzatti, G. Groppi, Catal. Today 54 (1999) 165.
[2] M.F.M. Zwinkels, S.G. Järås, P. Govin Menon, T.A. Griffin, Catal. Rev. Sci. Eng. 35 (1993) 319.
[3] G. Saracco, I. Cerri, V. Specchia, R. Accornero, Chem. Eng. Sci. 54 (1999) 3599.

[4] D. Klvana, J. Delval, J. Kirchnerova, J. Chaouri, Appl. Catal. A: Gen. 165 (1997) 171.
[5] I. Rosso, E. Garrone, F. Geobaldo, B. Onida, G. Saracco, Appl. Catal. B: Environ. 30 (2001) 61.
[6] P.G. Tsyrulnikov, O.N. Kovalenko, L.L. Gogin, T.G. Starostina, A.S. Noskov, A.V. Kalinkin, A.V. Krukova, S.V. Tsybulya, E.N. Kudrya, A.V. Bubnov, Appl. Catal. A: Gen. 167 (1998) 31.
[7] D. Ugues, S. Specchia, G. Saracco, Ind. Eng. Chem. Res. 43 (2004) (1990).
[8] S. Specchia, A. Civera, G. Saracco, Chem. Eng. Sci. 59 (2004) 5091.
[9] A. Civera, G. Negro, S. Specchia, G. Saracco, V. Specchia, Catal. Today 100 (2005) 275.
[10] S. Specchia, A. Civera, G. Saracco, V. Specchia, Catal. Today 117 (2006) 427.
[11] S. Specchia, M.A. Ahumada Irribarra, P. Palmisano, G. Saracco, V. Specchia, Ind. Eng. Chem. Res. 46 (2007) 6666.
[12] C.A. Müller, M. Maciejewski, R.A. Koeppel, A. Baiker, J. Catal. 166 (1997) 36.
[13] T. Seyama, Catal. Rev. Sci. Eng. 34 (1992) 281.
[14] S. Cimino, R. Pirone, L. Lisi, Appl. Catal. B: Environ. 35 (2002) 243.
[15] J.G. Mc Carty, H. Wise, Catal. Today 8 (1990) 231.
[16] R.J.V. Voorhoeve, D.W. Johnson Jr., D.P. Remeika, P.K. Gallagher, Science 195 (1977) 827.
[17] L.G. Tejuca, J.L.G. Fierro, J.M.D. Tascón, Adv. Catal. 36 (1989) 237.
[18] P. Palmisano, N. Russo, P. Fino, D. Fino, C. Badini, Appl. Catal. B: Environ. 69 (2006) 85.
[19] M. Boaro, M. Vicario, C. de Leitenburg, G. Dolcetti, A. Trovarelli, Catal. Today 77 (2003) 407.
[20] M.L. Pisarello, V. Milt, M. A: Peralta, E.E. Mirò, Catal. Today 75 (2002) 465.
[21] A.S. Mukasyanj, C. Costello, K.P. Sherlock, D. Lafarga, A. Varma, Sep. Purif. Technol. 25 (2001) 117.
[22] A. Civera, M. Pavese, G. Saracco, V. Specchia, Catal. Today 83 (2003) 199.
[23] B. Beguin, E. Garbowski, M. Primet, Appl. Catal. 75 (1991) 119.
[24] Y. Zhang-Steenwinkel, H.L. Castricum, J. Beckers, E. Eiser, A. Bliek, J. Catal. 221 (2004) 523.
[25] M. Alifanti, R. Auer, J. Kirchnerova, F. Thyrion, P. Grange, B. Delmon, Appl. Catal. B: Environ. 41 (2003) 71.
[26] V.A. de la Peña O'Shea, M.C. Alvarez-Galvan, J. Requies, V.L. Barrio, P.L. Arias, J.F. Cambra, M.B. Güemez, J.L.G. Fierro, Catal. Commun. 8 (2007) 1287.
[27] J. Hu, W. Chu, L. Shi, J. Nat. Gas Chem. 17 (2008) 159.
[28] J. Requies, M.C. Alvarez-Galvan, V.L. Barrio, P.L. Arias, J.F. Cambra, M.B. Güemez, A. Manrique Carrera, V.A. de la Peña O'Shea, J.L.G. Fierro, Appl. Catal. B: Environ. 79 (2008) 122.
[29] S.A. Yashnik, Z.R. Ismagilov, V.V. Kuznetsov, V.V. Ushakov, V.A. Rogov, I.A. Ovsyannikova, Catal. Today 117 (2006) 525.
[30] S. Cimino, S. Colonna, S. De Rossi, M. Faticanti, L. Lisi, I. Pettiti, P. Porta, J. Catal. 205 (2002) 309.
[31] D. Terribile, A. Trovarelli, C. de Leitenburg, A. Primavera, G. Dolcetti, Catal. Today 47 (1999) 133.
[32] L.V. Interrante, M.J. Hampden-Smith, Chemistry of Advanced Materials, Wiley, NY, 1998.
[33] Y. Teraoka, M. Yoshimatsu, N. Yamazoe, T. Seyama, Chem. Lett. (1984) 893.
[34] V. Sanchez Escribano, E. Fernandez Lopez, M. Panizza, C. Resini, J.M. Gallardo Amores, G. Busca, Solid State Sci. 5 (2003) 1369.
[35] E. Finocchio, G. Busca, P. Forzatti, G. Groppi, A. Beretta, Langmuir 23 (2007) 10419.
[36] M. Baldi, V. Sanchez Escribano, J.M. Gallardo Amores, F. Milella, G. Busca, Appl. Catal. B: Environ. 17 (1998) L175.
[37] M. Waquif, P. Bazin, O. Saur, J.C. Lavalley, G. Blanchard, O. Touret, Appl. Catal. B: Environ. 11 (1997) 193.
[38] T. Luo, R.J. Gore, Appl. Catal. B: Environ. 53 (2004) 77.
[39] L.J. Hoyos, Appl. Catal. A: Gen. 98 (1993) 125.
[40] I. Rosso, S. Fiorilli, B. Onida, G. Saracco, E. Garrone, J. Phys. Chem. B 106 (2002) 11980.
[41] C. Binet, M. Daturi, J.C. Lavalley, Catal. Today 50 (1999) 207.
[42] L. Zenboury, B. Azambre, J.V. Weber, Catal. Today 137 (2008) 167.